

Preparation of High-Activity MgO-Supported Co–Mo and Ni–Mo Sulfide Hydrodesulfurization Catalysts

T. Klicpera and M. Zdražil¹

Institute of Chemical Process Fundamentals, Academy of Sciences of the Czech Republic, Rozvojová 135, CZ-165 02, Prague 6-Suchbát, Czech Republic

Received September 4, 2001; revised November 21, 2001; accepted November 21, 2001; published online February 7, 2002

CoO–MoO₃/MgO and NiO–MoO₃/MgO catalysts were prepared from MoO₃/MgO by impregnation with methanol solutions of Co nitrate and Ni nitrate, respectively, followed by calcination at 350°C. The texture of the starting MoO₃/MgO was preserved during this preparation. The hydrodesulfurization activity of the pre-sulfided catalysts was evaluated using the reaction of benzothiophene (1.6 MPa, 300–360°C). Commercial CoMo/Al₂O₃ (Shell 344) and NiMo/Al₂O₃ (Shell 324) catalysts were used as reference points of activity. A strong synergistic effects in activity between Co(Ni) and Mo in Co(Ni)Mo/MgO catalysts was observed with an optimum Co(Ni)O content of about 3–4 wt%. The most active Co(Ni)Mo/MgO catalysts were 1.5 to 2.3 times more active than their corresponding Al₂O₃-supported counterparts. MgO should be considered a new promising support for Co(Ni)Mo sulfide catalysts. However, its sensitivity to water and propensity to form solid solutions with CoO and NiO must be taken into consideration in catalyst preparation. © 2002 Elsevier Science (USA)

Key Words: hydrodesulfurization; sulfide catalysts; MgO support; benzothiophene; synergistic effect.

1. INTRODUCTION

The catalysts used for hydrodesulfurization (HDS) of petroleum fractions are mixed Co–Mo or Ni–Mo sulfides supported on Al₂O₃. Strict regulation of the sulfur content in fuels is the driving force for further research and development of more active catalysts. One important direction of current research focuses on the support material. Active carbon, ZrO₂, TiO₂, zeolites, and various mixed oxides have been studied as alternatives for the conventional Al₂O₃ support (for review see Refs. (1–6)). All these supports are acidic or neutral and very limited attention has been devoted to basic supports. However, basic supports might be interesting for two main reasons. First, the acid–base interaction between acidic MoO₃ and a basic support in the oxidic precursor of sulfide catalysts should promote a high and stable dispersion of the Mo species. Second, the basic character of the support should inhibit coking which

is rather intensive over conventional Al₂O₃ supported catalysts (7).

The literature on Co- or Ni-promoted Mo/MgO sulfide catalysts is very limited. A patent (8) reported the preparation of a Co–Mo/MgO catalyst by drying and calcination of an aqueous slurry of Mg(OH)₂, Co(NO₃)₂, and (NH₄)₆Mo₇O₂₄. The HDS activity was tested for crude oil and lubricating oil at 10 MPa and 450°C. The initial activity of the Co–Mo/MgO catalyst was about the same as the activity of a Co–Mo/Al₂O₃ reference sample. However, catalyst deactivation was faster over the Al₂O₃-supported catalyst than over the MgO-supported catalyst. After 300 h on stream, the MgO-supported catalyst was about two to three times more active than the Al₂O₃-supported sample (in terms of pseudo first-order rate constants calculated from the conversions published in the patent).

Ramírez and colleagues (9) prepared Ni–Mo/MgO catalysts with various atomic ratios Ni/(Ni + Mo) by successive incipient wetness impregnation with aqueous solutions of (NH₄)₆Mo₇O₂₄ and Ni(NO₃)₂ with a final calcination at 500°C. The activity was tested in the HDS of thiophene. Practically no synergistic effect in activity between Ni and Mo at the atomic Ni/(Ni + Mo) ratio of 0.3 was observed, and this Ni–Mo/MgO catalyst was five times less active than a reference Ni–Mo/Al₂O₃ catalyst of the same composition. It was suggested that the majority of the Ni was deactivated by the formation of a NiO–MgO solid solution. At the Ni/(Ni + Mo) ratio of 0.6, a synergistic effect was observed in the Ni–Mo/MgO catalyst, but the activity of this catalyst was only about half that of its Al₂O₃-supported counterpart.

The method of preparation of high-surface-area MgO (200–300 m² g⁻¹) is well known (e.g., (10)). However, this material is very sensitive to water, and the conventional impregnation with an aqueous solution of a metal salt completely destroys its texture. For instance, the degree of hydration of MgO with surface area of 155 m² g⁻¹ to Mg(OH)₂ was 86% in an aqueous slurry after 15 min at 16°C (11). The hydration proceeds easily also during storage at ambient atmosphere. The mechanism of hydration is not penetration of water into the MgO structure, but

¹ To whom correspondence should be addressed. Fax: +420 2 20920661. E-mail: zdrazil@icpf.cas.cz.

a dissolution–precipitation (recrystallization) cycle (12). MgO is dissolved and new crystals of $\text{Mg}(\text{OH})_2$ grow, the texture of which is essentially independent of the texture of the starting MgO.

Our previous work concerned the preparation of MoO_3/MgO catalysts by nonaqueous impregnation (13–15). It was found that the texture of the starting high-surface-area MgO was stable in methanol and ethanol. The catalysts were prepared by the reaction of MgO with a slurry of $(\text{NH}_4)_6\text{Mo}_7\text{O}_{24}$ (13, 14) or MoO_3 (15) in these alcohols. The activity in the HDS of benzothiophene of the most active MoO_3/MgO samples was the same as the activity of a commercial $\text{MoO}_3/\text{Al}_2\text{O}_3$ catalyst.

The subject of the present work is the promotion of the above-mentioned highly active MoO_3/MgO catalyst by Co and Ni. The promoters were deposited from an alcoholic solution of their nitrates. Activity was tested using the HDS of benzothiophene. Commercial Co–Mo/ Al_2O_3 (Shell 344) and Ni–Mo/ Al_2O_3 (Shell 324) samples were used as reference catalysts.

2. EXPERIMENTAL

2.1. Catalyst Preparation

2.1.1. Catalysts supported over MgO of particle size 0.16–0.32 mm. MoO_3/MgO catalyst was prepared by reaction of MgO (particle size fraction 0.16–0.32 mm, surface areas $\text{SA}_{\text{s},350}$ and $\text{SA}_{\text{f},350}$ of 243 and 230 $\text{m}^2 \text{g}^{-1}$, respectively) with MoO_3 in a slurry in aqueous methanol (4 wt% of water) at room temperature for 10 days. Its nominal composition and the composition found by AAS analysis were 15 and 14.6 wt% MoO_3 , respectively. Its surface areas $\text{SA}_{\text{s},350}$ and $\text{SA}_{\text{f},350}$ were 235 and 228 $\text{m}^2 \text{g}^{-1}$, respectively. More details of its preparation and activity can be found elsewhere: the sample used refers to sample 15MoPart(am) in Ref. (15). It is designated as 15Mo/MgO in the present work.

CoO– MoO_3/MgO and NiO– MoO_3/MgO catalysts with various contents of CoO and NiO were prepared by impregnation of the above 15Mo/MgO catalyst with solutions of Co nitrate and Ni nitrate in methanol, respectively. The catalyst named 3.5Co15Mo/MgO was prepared by impregnation of the 15Mo/MgO catalyst and contained 3.5 wt% CoO. The 15Mo/MgO catalyst was recalcined immediately before impregnation (40 min at 350°C in flow of air). The concentration of the impregnation solution corresponded to 0.4 g of CoO or NiO per 100 ml of solution. The mixture was left standing at room temperature for 2 days and all Co nitrate or Ni nitrate adsorbed after that time (the solution decolorized). The mixture was dried in a rotary vacuum evaporator at 60°C until it became particulate and then the drying was continued at 100°C for 40 min. The catalyst was calcined in a tubular flow reactor in a stream of air for 40 min at 350°C.

CoO/MgO and NiO/MgO catalysts were prepared by impregnation of MgO (surface area $\text{SA}_{\text{s},350}$ of 245 $\text{m}^2 \text{g}^{-1}$, particle size fraction 0.16–0.32 mm) by the same procedure as described above. Catalyst 3Ni/MgO contained 3 wt% NiO.

2.1.2. Catalysts supported over MgO extrudates. The purpose of preparation of these samples by impregnation of MgO extrudates (diameter 2.6 mm, surface area $\text{SA}_{\text{s},350}$ of 250 $\text{m}^2 \text{g}^{-1}$) was to get information about the strength of adsorption of metal species deposited during impregnation. The formation of eggshell concentration profiles in the course of impregnation indicates very strong adsorption. The distribution of metals across the extrudates was evaluated by electron probe microanalysis. The samples were not tested for activity.

The catalyst 15Mo/MgO(E, MoO_3) supported on MgO extrudates was prepared by the procedure described above for the 15Mo/MgO catalyst supported over 0.16- to 0.32-mm MgO particles. The extrudate samples were removed after various impregnation times; all MoO_3 powder had disappeared after an impregnation time of 300 h.

5CoO/MgO(E) catalyst supported on MgO extrudates was prepared by the procedure described above for the Co(Ni)/MgO catalyst supported over 0.16- to 0.32-mm MgO particles.

3.5Co15Mo/MgO(E,AHM) catalyst was prepared by impregnation of MoO_3/MgO extrudates by the procedure described above for 3.5Co15Mo/MgO catalyst supported over 0.16- to 0.32-mm MoO_3/MgO particles. The starting MoO_3/MgO extrudates (nominal loading 15 wt% MoO_3) were prepared by reaction of the MgO extrudates with a slurry of ammonium heptamolybdate (AHM) in nonaqueous methanol as described in our previous work. The distribution of MoO_3 across the extrudates was uniform (14).

2.2. Hydrodesulfurization

HDS data were obtained in a fixed-bed tubular reactor (i.d. 2 mm) with the reaction mixture in the gas phase. The feed consisted of a solution of benzothiophene (BT) in decane (D) and the feed rates, F_i , of BT, D, and H_2 were 7.7, 89, and 595 mmol h^{-1} , respectively. The total pressure was 1.6 MPa and each catalyst charge W was tested consecutively at the reaction temperatures 330, 300, and 360°C. The catalyst charge was in the range 0.02–0.7 g and was diluted with inert corundum (0.16–0.32 mm). The products of the reaction were dihydrobenzothiophene (DHBT) and ethylbenzene (EB); the amount of other carbon-containing products was negligible. Results were evaluated in terms of relative reaction mixture composition, a_i , or conversion, x_i ($a_{\text{BT}} = n_{\text{BT}}/n_{\text{BT}}^0$, $a_{\text{DHBT}} = n_{\text{DHBT}}/n_{\text{BT}}^0$, $a_{\text{EB}} = n_{\text{EB}}/n_{\text{BT}}^0$); overall conversion of BT ($x_{\text{BT}} = 1 - a_{\text{BT}}$); conversion of BT to DHBT ($x_{\text{DHBT}} = a_{\text{DHBT}}$); and conversion of BT to EB ($x_{\text{EB}} = a_{\text{EB}}$), where n^0 and n are initial and final numbers of moles, respectively. The catalyst was presulfided *in situ* in

a flow of $\text{H}_2\text{S}/\text{H}_2$ (1/10) with a temperature ramp program of $8.4^\circ\text{C min}^{-1}$ to 400°C and a dwell time of 1 h at 400°C . Steady state of the outlet composition was achieved 20 min after each change of reaction conditions (start of feed or change of temperature) and no catalyst deactivation was observed during the test (the duration of the test at each temperature was about 1 h after steady state was attained).

2.3. Surface Area

The critical point of the measurement of high-surface-area MgO and of the related MgO-supported catalysts is the temperature of the *in situ* pretreatment. Evacuation of the sample at about $250\text{--}350^\circ\text{C}$ is generally used for alumina-supported catalysts in the measurement by the adsorption of N_2 by the static method. This relatively severe pretreatment is needed in the static method to achieve a high and stable vacuum. However, in the case of MgO-based samples, the cycle impregnation of the sample/*in situ* pretreatment at $250\text{--}350^\circ\text{C}$ may completely change the surface area as compared with the sample before impregnation. That is why surface area (SA) was measured in the present work by the adsorption of nitrogen using the dynamic flow method (16) which allows the measurement without any *in situ* pretreatment of the sample (immediately after drying in a rotary vacuum evaporator). The corresponding surface area is denoted $\text{SA}_{f,25}$. The surface area was also measured by the flow method after *in situ* pretreatment in a flow of air for 40 min at 350°C and is denoted $\text{SA}_{f,350}$. Selected samples were measured by the conventional static method (the complete N_2 adsorption isotherm was measured) using a Micromeritics ASAP 2010 instrument after *in situ* outgassing at 350°C *in vacuo*, and the values obtained are denoted $\text{SA}_{s,350}$.

2.4. Electron Probe Microanalysis

Distribution profiles of Mo and Co in extrudates were obtained using a JEOL JXA electron microscope equipped with the ED analyzer EDAX PV 9400.

3. RESULTS AND DISCUSSION

3.1. Surface Area

Impregnation of the MoO_3/MgO catalyst or MgO support by a methanol solution of Co(Ni) nitrate did not significantly change the surface area of the sample. $\text{SA}_{f,25}$ of the dried Co(Ni)–Mo/MgO and Co(Ni)/MgO samples was about the same ($\pm 10\%$) as the surface area of the starting material. $\text{SA}_{f,350}$ was about 10% higher than the corresponding value of $\text{SA}_{f,25}$. For instance, the $\text{SA}_{f,350}$ of the starting MoO_3/MgO particles was $228\text{ m}^2\text{ g}^{-1}$ and $\text{SA}_{f,25}$ and $\text{SA}_{f,350}$ of $3\text{Ni}15\text{Mo}/\text{MgO}$ were 220 and $245\text{ m}^2\text{ g}^{-1}$, respectively.

3.2. Distribution of Co(Ni) and Mo Species in Catalyst Particles

It should be expected that the interaction of acidic MoO_3 and Co(Ni) nitrates with basic MgO is rather strong. This may result in an uneven distribution of Mo and Co(Ni) species even when MgO and $15\text{Mo}/\text{MgO}$ samples with a particle size of $0.16\text{--}0.32\text{ mm}$ were impregnated. Measurement of the distribution in such small particles is experimentally difficult. For that reason, the situation was clarified by experiments with extrudates and the results are shown in Fig. 1.

$15\text{Mo}/\text{MgO}(\text{E},\text{MoO}_3)$ catalyst was prepared by impregnation of MgO extrudates by the same method as used for the impregnation of $0.16\text{--}0.32\text{-mm}$ MgO particles (slurry of MoO_3 and MgO in aqueous methanol at room temperature). An eggshell profile of the MoO_3 concentration was obtained, indicating that the interaction of MoO_3 with MgO was strong. The depth of the profile was about 0.5 mm after an impregnation time of 240 h when all powdered MoO_3 had disappeared from the mixture. However, the starting $15\text{Mo}/\text{MgO}$ catalyst used for promotion by Co(Ni) was prepared by impregnation of $0.16\text{--}0.32\text{-mm}$ MgO particles and it can be concluded that these small particles have a uniform MoO_3 distribution.

A sharp eggshell profile with a mean depth of about 0.2 mm was obtained for the $5\text{Co}/\text{MgO}(\text{E})$ catalyst. The height of this profile was about 10 wt% CoO. It cannot be excluded that the distribution of CoO obtained by impregnation of the $0.16\text{--}0.32\text{-mm}$ MgO particles was not completely uniform. The purpose of the preparation of the Co(Ni)/MgO samples (particle size $0.16\text{--}0.32\text{ mm}$) was measurement of their HDS activity for evaluation of the synergistic effect in Co(Ni)Mo/MgO catalysts (see Section 3.4.3). An unevenness of Co(Ni) distribution might have an effect on HDS activity. However, the activity of Co(Ni)/MgO was lower than that of Mo/MgO and it was assumed that the effect of possible nonuniform Co(Ni) distribution in the Co(Ni)/MgO catalysts on evaluation of the synergistic effect was negligible.

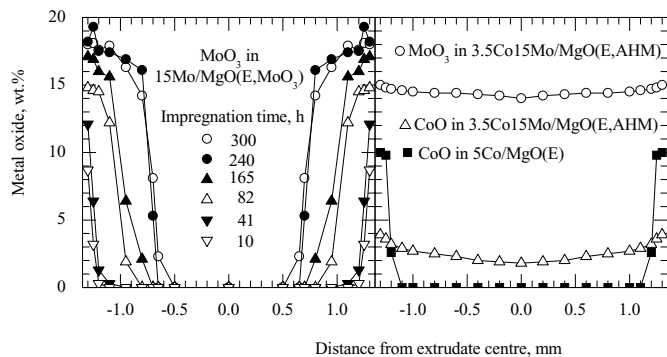


FIG. 1. Distribution of metal oxides in catalysts supported over MgO extrudates.

The starting MoO_3/MgO extrudates for preparation of the $3.5\text{Co}15\text{Mo}/\text{MgO}(\text{E,AHM})$ catalyst were prepared by reaction of neutral ammonium heptamolybdate with MgO extrudates in methanol at room temperature and had a uniform distribution of MoO_3 (14). The data in Fig. 1 confirm that this uniform distribution of MoO_3 did not change during deposition of CoO . Deposited MoO_3 neutralized the basic MgO , and the interaction of Co nitrate with the surface of MoO_3/MgO was weaker than that with MgO . A uniform profile of CoO concentration across the extrudate was obtained in the $3.5\text{Co}15\text{Mo}/\text{MgO}(\text{E,AHM})$ catalyst. This proved that the distribution of $\text{Co}(\text{Ni})\text{O}$ in the promoted catalysts obtained by impregnation of $15\text{Mo}/\text{MgO}$ catalyst of particle size fraction $0.16\text{--}0.32$ mm was also uniform.

3.3. Evaluation of HDS Activity

3.3.1. Kinetic scheme. The integral dependencies of a_{BT} , a_{DHBT} , and a_{EB} versus space time W/F_{BT} were measured for four selected catalysts: $3\text{Ni}15\text{Mo}/\text{MgO}$, $3.5\text{Co}15\text{Mo}/\text{MgO}$, $3.5\text{Ni}19\text{Mo}/\text{Al}_2\text{O}_3$ (Shell 324), and $3.5\text{Co}15\text{Mo}/\text{Al}_2\text{O}_3$ (Shell 344). Examples of these dependencies are shown in Fig. 2. The data were well fitted by a parallel-consecutive scheme of four pseudo-first-order reactions (BT to DHBT, DHBT to BT, BT to EB, and DHBT to EB).

3.3.2. Selectivity to DHBT. The synergistic effect in the HDS activity of bimetallic sulfide catalysts is generally accompanied by a characteristic change in the distribution of the intermediates. By combining $\text{Co}(\text{Ni})$ and $\text{Mo}(\text{W})$ in the catalyst, the rates of the hydrogenolytic steps (the steps consuming H_2 with breaking of the C–S bond) are more accelerated than the hydrogenation steps (the steps consuming H_2 without breaking of the C–S bond). This phenomenon is related to active phase and was observed for both the unsupported sulfides and the sulfides supported on various supports (for review see Refs. (17–20), for recent original papers see Refs. (21–25)). Practically no previous data

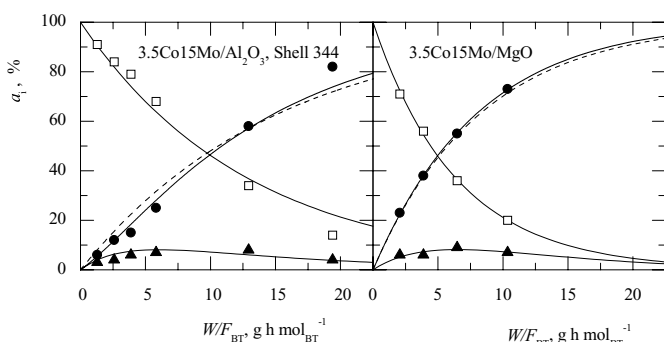


FIG. 2. Dependence of reaction mixture composition on space time in hydrodesulfurization of benzothiophene at 300°C . Open squares: a_{BT} , full triangles: a_{DHBT} , full circles: a_{EB} , solid lines: obtained by fitting using four-constant reaction scheme, dashed lines: fitted by first-order equation (the constants are shown in Table 1).

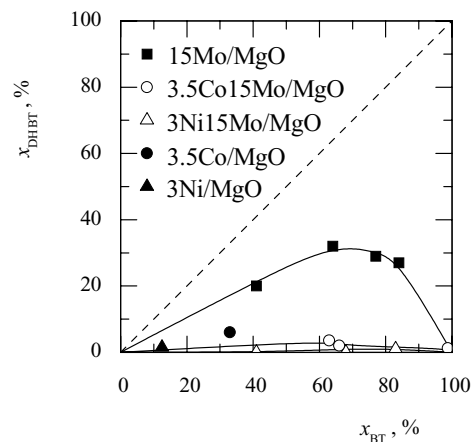


FIG. 3. Selectivity to intermediate dihydrobenzothiophene (DHBT) during hydrodesulfurization of benzothiophene (BT) at 330°C . The dashed line represents the stoichiometric limitation of x_{DHBT} .

are available for MgO -supported catalysts and our results shown in Fig. 3 confirm that the above rule also holds for this support. Dihydrobenzothiophene is formed by hydrogenation and removed by hydrogenolysis and the synergism in activity of $\text{Co}(\text{Ni})\text{Mo}/\text{MgO}$ catalysts was accompanied by a sharp decrease in the selectivity to this intermediate. The data obtained at 330°C are shown in Fig. 3; the data obtained at 300 and 360°C exhibited analogous features.

3.3.3. Index of the overall HDS activity. The integral curves of the conversions x_i versus space time W/F_{BT} could be fitted well by a scheme of four pseudo-first-order rate equations (see Section 3.3.1). The values of these constants are not presented because none of them is a proper index of overall HDS activity (it is also not possible to combine them into a single activity parameter). However, it was found that the disappearance of BT and formation of EB can be described by first-order rate equations in good approximation, as illustrated by the dashed lines for EB formation in Fig. 2. The corresponding rate constants are named k_{BT} and k_{EB} , respectively. (The data for the Shell 344 catalyst in Fig. 2 could also be fitted by a zero-order rate equation; however, the point at $W/F_{\text{BT}} = 19.4$ g h mol^{-1} was clearly measured with a large error because all our previous data concerning various $\text{Co}(\text{Ni})\text{Mo}/\text{Al}_2\text{O}_3$ -supported samples (26, 27) were much better fitted by a first-order than a zero-order equation.)

The ranking of catalysts of the same type (all nonpromoted or all promoted catalysts) is the same according to BT disappearance or EB formation, because selectivity to DHBT is the same for each catalyst type. However, nonpromoted and promoted catalysts differ strongly in selectivity to DHBT (see Section 3.3.2) and their relative activities differ to some extent according to k_{BT} and k_{EB} .

Two indices of overall HDS activity were used. The effects of calcination temperature and of promoter

concentration on activity were tested using the conversion of BT to EB, x_{EB} , at fixed space time W/F_{BT} as an activity index. The synergistic effect, *SYN*, and the comparison of MgO- and Al₂O₃-supported catalysts were evaluated in terms of k_{EB} ($SYN = k_{EB}(\text{Co(Ni)Mo}) / (k_{EB}(\text{Co(Ni)}) + k_{EB}(\text{Mo}))$).

3.4. HDS Activity

3.4.1. Effect of calcination. A solid solution of Co(Ni)O–MgO is easily formed by heating Co(Ni)O and MgO. Ramírez and colleagues (9) concluded that the loss of supported Ni species by formation of a solid solution with the MgO support during calcination of their NiMo/MgO catalysts (24 h at 500°C) significantly reduced HDS activity. The effect of calcination temperature was tested with the 3Ni15Mo/MgO catalyst in the present work. The conversion x_{EB} at a space time W/F_{BT} of 6.47 g h mol⁻¹ and HDS temperature of 300°C of the samples calcined at 250 and 350°C was 43 and 45%, respectively. However, a sharp decrease in activity was observed after calcination at 400°C; x_{EB} was only 16% for this sample. The temperature of 350°C was therefore selected as the standard calcination temperature.

3.4.2. Effect of Co(Ni)O loading. 15Mo/MgO catalyst was impregnated with various amounts of Co and Ni and the samples were tested for their HDS activity (x_{EB} at fixed space time W/F_{BT}). The results are shown in Fig. 4. A strong promotion effect was observed that was stronger for Co–Mo than for Ni–Mo catalysts. The optimum concentration of the promoters was about 3–4 wt% CoO or NiO. The corresponding Co(Ni)O/MoO₃ ratio corresponds well to the usual ratio of these oxides in industrial Al₂O₃-supported catalysts. The synergistic effect in the most active catalysts of Fig. 4 is discussed below in terms of rate constants k_{EB} . However, the description of the synergistic effect in terms of conversions under fixed kinetic conditions is very illustrative and two important points should be mentioned in connection with Fig. 4.

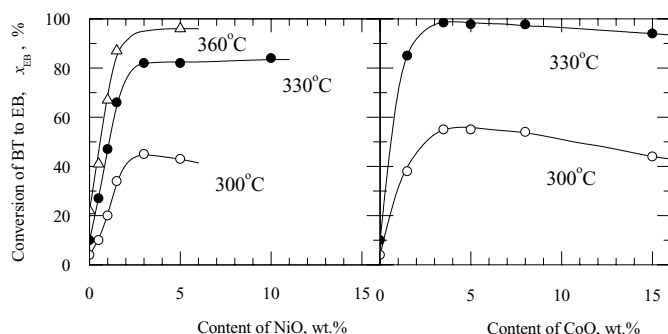


FIG. 4. Dependence of the conversion of benzothiophene (BT) to ethylbenzene (EB) on Co(Ni)O content of the Co(Ni)15Mo/MgO catalyst. Space time W/F_{BT} was 6.47 g · h mol⁻¹.

i. The promotion effect for MgO-supported catalysts seems to be very strong as compared with other supports. This point is discussed more in detail in Section 3.4.3.

ii. The large promotion effect over MgO-supported catalysts observed in the present work is at variance with the work of Ramírez and colleagues (9). The atomic ratio Co(Ni)/(Co(Ni) + Mo) in our work was about 0.3 and Ramírez *et al.* observed essentially no promotion at this composition; they observed some promotion only when the ratio Ni/(Ni + Mo) was increased to 0.4 and 0.6. This contradiction can be explained by two factors. First, Ramírez and colleagues calcined their catalysts for 24 h at 500°C and concluded that most of the nickel is lost by formation of a solid NiO–MgO solution. In the present work, the samples were calcined at 350°C for 40 min and it was shown above that, a higher calcination temperature lowered the activity of the final catalyst. It is concluded that the low calcination temperature prevents the formation of a solid NiO–MgO solution. Second, the surface area of the MoO₃/MgO catalysts was preserved in our nonaqueous impregnation. On the other hand, the strong decrease in surface area as found by Ramírez *et al.* suggests that a complete chemical and textural reconstruction of the starting MoO₃/MgO catalyst occurred during aqueous impregnation (for instance, the surface area of their MoO₃/MgO of 329 m² g⁻¹ decreased to 154 m² g⁻¹ for the NiO–MoO₃/MgO sample).

3.4.3. Synergistic effect between Co(Ni) and Mo in the overall HDS activity. The synergistic effect *SYN* was evaluated in terms of k_{EB} as the ratio $k_{EB}(\text{Co(Ni)Mo}) / (k_{EB}(\text{Co(Ni)}) + k_{EB}(\text{Mo}))$. The constants k_{EB} for the Co(Ni)Mo/MgO and Co(Ni)Mo/Al₂O₃ samples were evaluated by fitting the dependencies x_{EB} versus space time W/F_{BT} , as discussed in Section 3.3.3. For the Mo/MgO and Mo/Al₂O₃ catalysts they were obtained by fitting these dependencies measured in our previous work (13–15). For the Co(Ni)/MgO samples, only conversions at one value of space time W/F_{BT} were measured in the present article, and the constants k_{EB} were calculated (no fitting) by using a pseudo-first-order rate equation. The results are summarized in Table 1.

It follows from the data in Table 1 that the activity per mole of metal of the Co/MgO and Ni/MgO catalysts is of the same order of magnitude as the activity of the Mo/MgO sample. This agrees with the data reported in the literature for Al₂O₃-supported catalysts (28, 29). However, Table 1 shows that combining Co(Ni) and Mo in MgO-supported catalysts resulted in an increase in the activity of one order of magnitude. The synergistic effect was about 20. Such strong synergism has not been reported for MgO-supported catalysts up to now.

In our experience, two conditions must be fulfilled to achieve strong synergism over MgO-supported catalysts. (i) The Co or Ni promoters must be deposited by a method that does not change the chemical structure and texture of

TABLE 1
Comparison of MgO- and Al₂O₃-Supported Catalysts with Respect to HDS Activity and Synergistic Effect SYN

Catalyst	k_{EB} (mmol g ⁻¹ h ⁻¹)			SYN ^a		
	300°C	330°C	360°C	300°C	330°C	360°C
CoMo/MgO system						
3.5Co/MgO	1.3	3.1	6.4			
15Mo/MgO	4.8	13.7	32.7			
3.5Co15Mo/MgO	124	461	—	20	27	—
NiMo/MgO system						
3Ni/MgO	0.5	1.0	2.1			
15Mo/MgO	4.8	13.7	32.7			
3Ni15Mo/MgO	104	295	527	20	20	15
Reference Al ₂ O ₃ -supported systems						
15Mo/Al ₂ O ₃ (BASF M8-30)	4.5	14.9	34.3			
3.5Ni19Mo/Al ₂ O ₃ (Shell 324)	44.6	194	361	10	13	11
3.5Co15Mo/Al ₂ O ₃ (Shell 344)	65.5	198	479	15	13	14

^a For MgO-supported catalysts $SYN = k_{EB}(Co(Ni) - Mo) / (k_{EB}(Co(Ni)) + k_{EB}(Mo))$; for Al₂O₃-supported catalysts $SYN = k_{EB}(Co(Ni) - Mo) / k_{EB}(Mo)$.

the starting MoO₃/MgO catalyst. Explicitly, the dissolution of Mo species as MgMoO₄ and the hydration of MgO must be avoided. In our case, impregnation with a methanol solution was used, but it is expected that alternative methods can be developed. (ii) The promoted catalysts should not be calcined above 300–350°C because part of the promoter will be lost in the bulk of the MgO at higher temperatures.

We have made an attempt to compare the observed synergistic effect for MgO-supported catalysts with literature data concerning other supports. As for Al₂O₃-supported catalysts, some literature data are summarized in Refs. (5, 18) and it is concluded that the synergistic effect is mostly in the range 5–15. The values listed for Al₂O₃-supported catalysts in Table 1 also fall into this range (the ratio $k_{EB}(Co(Ni)-Mo)/k_{EB}(Mo)$ for commercial samples in Table 1 provides a reasonable judgment of synergism even when the Mo and Co(Ni) catalysts have a different origin). However, an even higher synergistic effect has been observed; e.g., Robinson *et al.* (30) reported values of about 30–40 for the NiMo/Al₂O₃ system (depending on the method of preparation). For ZrO₂-supported catalysts, synergism in the NiMo system was much lower than for Al₂O₃-supported catalysts, the values being 3 and 15, respectively (31). Also, for ZrO₂ stabilized by Y₂O₃ (3 mol%), synergism in the NiMo system was lower than with the Al₂O₃ support; the values were 8 and 13, respectively (32). For active carbon-supported catalysts, the recently reported values for the synergistic effect in the CoMo system are 10–15 (depending on the preparation method) (33) and 10 (34). It can be concluded that the synergistic effect observed in the present study for Co(Ni)Mo/MgO catalysts falls in the range of the highest values of synergism reported in the literature for Al₂O₃ and active carbon-supported catalysts.

It is well proved that synergism is connected to the deposition of Co(Ni) species onto edge planes of MoS₂ crystals (see Ref. (5)). It is speculated that the high synergistic effect observed in the present work for MgO-supported catalysts may be related to the basicity of the support. The edge planes of MoS₂ slabs possess Lewis acidity and the acid–base interaction with MgO probably promotes high dispersion of MoS₂ and inhibits the growth of MoS₂ crystals in the direction of the basal plane. This results in an increase in the ratio of surface edge planes to basal planes and, thus, in an increase in sites available for promotion.

3.4.4. Comparison of MgO- and Al₂O₃-supported catalysts. The activity data in Table 1 show that the MgO-supported Co(Ni)–Mo catalysts were 1.5–2.3 times more active than their Al₂O₃-supported commercial counterparts (depending on catalyst and reaction temperature). The activities of the parent Mo/MgO and Mo/Al₂O₃ catalysts were about the same, and the above high activity of the Co(Ni)–Mo/MgO samples is thus related to a strong synergism in the MgO-supported catalysts.

4. CONCLUSIONS

A strong synergistic effect between Co(Ni) and Mo was observed in the HDS activity of MgO-supported Co(Ni)–Mo sulfide catalysts. Co(Ni)Mo/MgO samples exhibited about 1.5–2.3 times higher activity in the HDS of benzothiophene than the corresponding reference commercial Al₂O₃-supported catalysts. This proves that very active Co(Ni)–Mo sulfide structures can be created under proper conditions on a MgO support. However, conventional aqueous impregnation and high calcination temperatures of 400–500°C, commonly used for Al₂O₃-supported

catalysts, are not suitable for MgO. High-surface-area MgO is chemically and texturally unstable in aqueous solutions and CoO and NiO oxides have the propensity to form a solid solution with MgO at high calcination temperature. In the present work, catalysts were prepared using methanol as solvent and at the low calcination temperature of 350°C. The high activity of the MgO-supported catalysts is an invitation for further research on the characterization of high-activity Co(Ni)Mo/MgO structures and on their preparation by a more practical method not including methanol.

ACKNOWLEDGMENTS

The authors thank Shell B.V. company for providing the samples of commercial catalysts. Support by the Grant Agency of the Czech Republic (Grant 104/01/0544) is gratefully acknowledged.

REFERENCES

- Luck, F., *Bull. Soc. Chim. Belg.* **100**, 781 (1991).
- Breyse, M., Portefaix, J. L., and Vrinat, M., *Catal. Today* **10**, 489 (1991).
- Delmon, B., *Catal. Lett.* **22**, 1 (1993).
- Vasudevan, P. T., and Fierro, J. L. G., *Catal. Rev.-Sci. Eng.* **38**, 161 (1996).
- Topsøe, H., Clausen, B. S., and Massoth, F. E., "Hydrotreating Catalysis, Science and Technology." Springer-Verlag, Berlin, 1996.
- Radovic, L. R., and Rodrigues-Reinoso, F., in "Chemistry and Physics of Carbon," Vol. 25: "Carbon Materials in Catalysis" (P. A. Thrower, Ed.), p. 243. Dekker, New York, 1997.
- Furimsky, E., and Massoth, F. E., *Catal. Today* **52**, 381 (1999).
- Kurokawa, S., and Miyasaki, T., Japanese Patent 75, 114 405 (1975). *Chem. Abstr.* **84**, 47020f (1975).
- Klimova, T., Casados, D. S., and Ramírez, J., *Catal. Today* **43**, 135 (1998).
- Holt, T. E., Logan, A. D., Chakraborti, S., and Datye, A. K., *Appl. Catal.* **34**, 199 (1987).
- Maryška, M., and Bláha, J., *Ceramics-Silikáty* **41**, 121 (1997).
- Mejias, J. A., Berry, A. J., Refson, K., and Fraser, D. G., *Chem. Phys. Lett.* **314**, 558 (1999).
- Klicpera, T., and Zdražil, M., *Catal. Lett.* **58**, 47 (1999).
- Klicpera, T., and Zdražil, M., *J. Mater. Chem.* **10**, 1603 (2000).
- Klicpera, T., and Zdražil, M., *Appl. Catal. A* **216**, 41 (2001).
- Nelsen, F. M., and Eggertsen, F. T., *Anal. Chem.* **30**, 1387 (1958).
- Zdražil, M., and Kraus, M., *Stud. Surf. Sci. Catal.* **27**, 257 (1986).
- Zdražil, M., *Catal. Today* **3**, 269 (1988).
- Zdražil, M., *Bull. Soc. Chim. Belg.* **100**, 769 (1991).
- Zdražil, M., in "Transition Metal Sulphides, Chemistry and Catalysis" (T. Weber, R. Prins, and R. A. van Santen, Eds.), NATO Advanced Science Institute Series, 3: High Technology, Vol. 60, p. 273. Kluwer, Dordrecht, 1998.
- Inamura, K., and Prins, R., *J. Catal.* **147**, 515 (1994).
- Taniguchi, M., Inamura, D., Ishige, H., Ishii, Y., Murata, T., Hidai, M., and Tatsumi, T., *J. Catal.* **187**, 139 (1999).
- Bataille, F., Lambertson, J. L., Michaud, P., Pérot, G., Vrinat, M., Lemaire, M., Schulz, E., Breyse, M., and Kasztelan, S., *J. Catal.* **191**, 409 (2000).
- Miller, J. T., Reagan, W. J., Kaduk, J. A., Marshall, C. L., and Kropf, A. J., *J. Catal.* **193**, 123 (2000).
- Bataille, F., Lambertson, J. L., Pérot, G., Leyrit, P., Cseri, T., Marchal, N., and Kasztelan, S., *Appl. Catal. A* **220**, 191 (2001).
- Peter, R., and Zdražil, M., *Collect. Czech. Chem. Commun.* **51**, 327 (1985).
- Fišer, J., Gulková, D., and Zdražil, M., *Bulg. Chem. Commun.* **30**, 168 (1998).
- Ahuja, S. A., Derrien, M. L., and Le Page, J. F., *Ind. Eng. Chem. Prod. Res. Dev.* **9**, 272 (1970).
- Wakabayashi, K., and Orito, Y., *Kogyo Kagaku Zasshi* **74**, 1317 (1971).
- Robinson, W. R. A. M., van Veen, J. A. R., de Beer, V. H. J., and van Santen, R. A., *Fuel Process. Technol.* **61**, 89 (1999).
- Duchet, J. C., Tilliet, M. J., Cornet, D., Vivier, L., Perot, G., Bekakra, L., Moreau, C., and Szabo, C., *Catal. Today* **10**, 579 (1991).
- Vrinat, M., Hamon, D., Breyse, M., Durand, B., and des Courieres, T., *Catal. Today* **20**, 273 (1994).
- Farag, H., Whitehurst, D. D., and Mochida, I., *Ind. Eng. Chem. Res.* **37**, 3533 (1998).
- Kaluža, L., and Zdražil, M., *Carbon* **39**, 2023 (2001).